PHYSICAL REVIEW B VOLUME 26, NUMBER 4 15 AUGUST 1982

# Screening effects in the core-level spectra of mixed-valence compounds

S.-J. Oh*
*Department of Physics, Stanford University, Stanford, California 94305*

S. Doniach
*Department of Applied Physics, Stanford University, Stanford, California 94305*
(Received 8 March 1982)

The effects of screening in the core-level photoemission spectra of mixed-valence compounds are studied with the use of an Anderson-model formulation. The mixed-valent ground-state properties and core-hole Green's function are calculated with the use of a decoupling approximation. The relative weights of peaks corresponding to two different configurations ($f^n$ and $f^{n+1}$) are found to become appreciably different from the ground-state valence due to shakedown as the hybridization between the localized $f$-level and conduction electrons is increased. The discrepancy is estimated to be of the order of $V/U_{df}$, where $U_{df}$ is the correlation energy between the core hole and $f$ electron, and $V$ represents the hybridization between $f$ electron and conduction electrons. We also find a shakedown $f^{n+2}$ peak in this limit. From a comparison of ground-state valence with the measured intensity of the shake-down peak for $CePd_3$, the width of the $f$ level due to hybridization is estimated to be of the order of 1 eV, in agreement with a recent resonant photoemission measurement.

## I. INTRODUCTION

Photoemission spectroscopy has proved to be a very powerful technique with which to study mixed-valence compounds. Valence-band photoemission has been used directly to estimate the position and width of an $f$ level relative to the Fermi level,[1-3] and this determination has recently become more unambiguous through the use of resonant photoemission.[4,5] X-ray photoemission from core levels of rare-earth compounds, $3d$ and $4d$ levels in particular, shows "fingerprint" multiplet structures resulting from different electronic configurations, and, in the case of mixed-valence compounds, two structures corresponding to $f^n$ and $f^{n+1}$ configurations may often be seen in the spectra.[1-3] The appearance of these structures was believed to be one of the clear tests to determine whether a particular compound is mixed valent or not. However, it was realized by many workers that the core-level x-ray photoemission spectroscopy (XPS) data may not reflect the initial-state configuration directly because of the strong disturbance a core hole makes on the system, and that final-state effects may play an important role.[6] In fact, it has been known for some time that the core-level spectra of some lanthanide compounds contain so-called "shake-up" and "shake-down" peaks as a result of final-state interaction.[7,8]

The final-state effect in the core-level photoemission spectra, especially in mixed-valence compounds, has become even more interesting in view of a recent suggestion by Wohlleben that there exist no tetravalent Ce compounds.[9] Available XPS core-level data on some of the standard "tetravalent" Ce compounds,[10] at first sight, seem to support this suggestion. For example, the $3d$ core-level XPS spectra of $CeRh_3$, which was believed to be of the $f^0$ configuration in the ground state, shows a structure corresponding to the $f^1$ configuration. Whether this is due to the final-state effect of a core hole or whether the $f^1$ configuration really exists in the ground state still remains open to discussion. To settle this issue we need a better understanding of final-state effects in mixed-valent systems. In this paper, we report an investigation of these effects and, in particular, of the effects of screening on the core-level photoemission spectra of metallic mixed-valent compounds.

Screening in the core-level spectra of metals is an interesting problem in itself, apart from the question of the mixed valency, and has been studied actively. Toyozawa and Kotani[11] (TK) intro-

duced an Anderson-model picture in which a local $d$ level is unoccupied in the ground state (i.e., is above the Fermi level) but becomes "pulled down" below the Fermi level by the core-hole potential, so that there is a finite probability of the $d$ level becoming occupied in the final state. The analysis of this model was later extended by Schönhammer and Gunnarsson[12] (SG). In a more detailed calculation, Lang and Williams[13] showed how the screening of a core hole by occupation of a localized level for a simple jellium situation could lead to a lower final-state energy than screening by image charges (plasmons). Gadzuk and Doniach[14] discussed the effect of this competition on the final-state probability distribution through the use of a very simplified model (see also Hussain and Newns[15]).

In the Anderson-type model, the empty screening level $|\phi_i\rangle$ (which we will think of as an $f$ level) is basically characterized by its position $\epsilon_f$ relative to the Fermi level $E_F$ and its coupling to the delocalized conduction-band electrons. The $f$-level energy $\epsilon_f$ is above $E_F$ in the initial state, but the Coulomb interaction of a core hole pulls it below $E_F$ in the final state. The total energy of the final state will thus be lowered if an electron is transferred from $E_F$ to the screening level $|\phi_i\rangle$. The probability of transferring an electron to the screening level $|\phi_i\rangle$ becomes bigger as the coupling of $|\phi_i\rangle$ to the conduction band is increased, hence, transferring spectral weight from the "unscreened" peak having unoccupied $|\phi_i\rangle$ to the "well-screened" peak with occupied $|\phi_i\rangle$. There seems to be experimental support for the usefulness of this picture. Fuggle *et al.*[16] observed that the intensity of the so-called well-screened peak compared to the unscreened peak descreases as the degree of localization of $|\phi_i\rangle$ is increased for a large class of transition-metal and rare-earth compounds.

In mixed-valent compounds the $f$ level is close to the Fermi level, so that its occupation may be expected to change on removal of a core electron leading to the above localized screening effect. However, in contrast to the situation discussed by earlier authors, the mixing of the occupancy of the $f$ level in the initial ground state cannot be neglected since we are interested in the mixed-valent case. Hence, the spectral weight of final states of various occupancy results partly from the mixing of occupancies in the initial state and partly from differing occupancy in final states, depending on the effectiveness of the above screening mechanism.

To deal with this situation, we have extended the relaxation calculations of TK and SG to the case where the initial state combines occupied and unoccupied configurations for the localized $f$ level. In order to work in a regime ($V_{kf} < U_{ff}$) close to the atomic limit, of relevance to rare-earth materials, our calculations are based on a Green's-function decoupling method introduced by Hewson[17] to discuss the localized impurity problem in which the atomic limit ($V_{kf} \to 0$) is treated exactly. Nevertheless, this technique involves an uncontrolled approximation (originally introduced in this context by Hubbard[18]), so the results may only be used to provide a qualitative guide to the physics involved.

## II. MODEL AND BASIC FORMALISM

### A. Anderson Hamiltonian and Green's function

The model Hamiltonian we use is a single-impurity Anderson-type Hamiltonian described by

$$H = \epsilon_d n_d + [\epsilon_f + U_{df}(1-n_d)] \sum_\sigma n_{f\sigma} + \sum_k \epsilon_k n_k + U_{ff} n_{f\sigma} n_{f-\sigma} + \sum_{k,\sigma} V_{kf}(a^\dagger_{k\sigma} a_{f\sigma} + a^\dagger_{f\sigma} a_{k\sigma}) , \quad (1)$$

where $\epsilon_d$ is the energy of the rare-earth core level ($3d$ or $4d$ level), $\epsilon_f$ is the energy of the $4f$ level which couples to the $5d\,6s$ conduction electrons via the hybridization $V_{kf}$. $U_{ff}$ is the intra-atomic Coulomb repulsion between two $4f$ electrons and $U_{df}(<0)$, the Coulomb attraction between the core hole and the localized $4f$ level, which is responsible for the pulling down of the $4f$ energy level in the final state. $\sigma$ represents the spin index.

The "effective" $f$-electron energy levels in the initial and final states of the Hamiltonian (1) are schematically shown in Fig. 1. This Hamiltonian was used by TK and SG to study the relaxation of a core hole in metals with an unoccupied valence level. The same Hamiltonian with $n_d = 1$ is also commonly used to model the ground-state valence-band electronic structures of mixed-valence materials. Through the use of a single-impurity model, we neglect the effects of the periodic lattice structure of mixed-valence compounds, but since the core-level photoionization is essentially a local event, we believe this will not change the basic physics of the problem. A more serious defect of this model to describe photoemission of real mixed-valence compounds such as $CePd_3$ may be the neglect of 14-fold degeneracy of the $4f$ level. We plan to look into this aspect of the problem in the future.

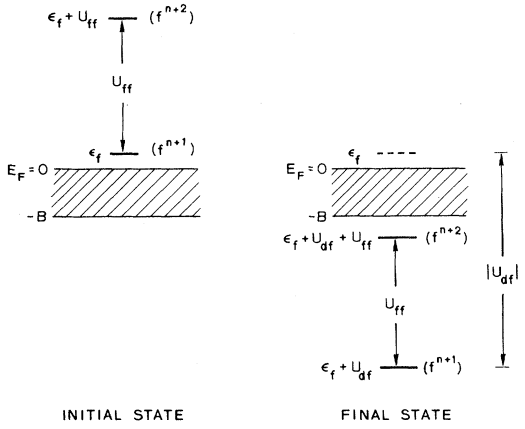


FIG. 1. "Effective" energy-level diagrams of $f$ levels in the initial and final states.

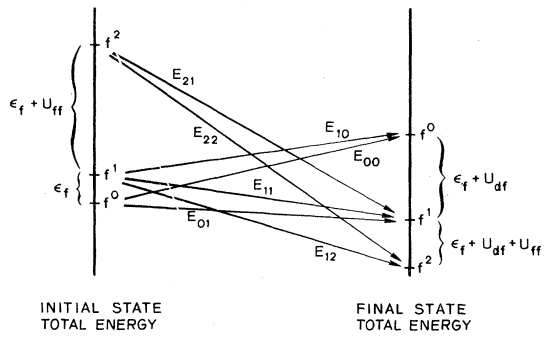


FIG. 2. Possible virtual transitions (shake-up and shake-down) near the atomic limit.

In x-ray photoemission spectra, the photoelectron current is proportional to the imaginary part of the Fourier transform of the retarded core-hole Green's function[18,19]

$$G_{dd}^R(t) \equiv \langle\langle a_d(t); a_d^\dagger(0) \rangle\rangle \equiv -i\Theta(t)\langle \{a_d(t), a_d^\dagger(0)\} \rangle , \quad (2)$$

where $\langle\ \rangle$ represents the ground-state expectation value, $\{\ \}$ the anticommutator, and $a_d(t)$ is a Heisenberg operator. If we assume no interaction between outgoing photoelectrons and the solid left behind, the cross section can be written as[20]

$$\frac{d^2\sigma}{d\omega\, d\epsilon_k} = -|M|^2 \frac{1}{\pi} \mathrm{Im} G_{dd}(\epsilon_k - \hbar\omega_q) , \quad (3)$$

where $G_{dd}(\omega)$ is the Fourier transform of $G_{dd}^R(t)$, $M$ the photoemission matrix element, $\hbar\omega_q$ the incident photon energy, and $\epsilon_k$ the outgoing photoelectron energy.

To gain some physical insight into the problem, we start by looking at the atomic limit $V_{kf}=0$ but assume we have an initial wave function which mixes all three configurations $n_f=1,2,3$ of $f$ occupancy. Since $V_{kf}=0$, there will be no change of occupancy on going to the final state and we see that

$$G_{dd}(\omega) = \frac{1-\sum_\sigma \langle n_{f\sigma}\rangle + \langle n_{f\sigma} n_{f-\sigma}\rangle}{\omega - \epsilon_d} + \frac{\sum_\sigma (\langle f_{f\sigma}\rangle - \langle n_{f\sigma} n_{f-\sigma}\rangle)}{\omega - \epsilon_d + U_{df}} + \frac{\langle n_{f\sigma} n_{f-\sigma}\rangle}{\omega - \epsilon_d + 2U_{df}} , \quad (4)$$

giving rise to three photoemission lines whose weight exactly measures the ground-state valency. This is the "spectator-hole" limit which has often been used in the interpretation of XPS data for mixed-valence materials.

In order to give a physical picture of the calculations which follow, we now consider what happens for very small but finite $V_{kf}$. The initial state is a mixture of four atomic limit states

$$\begin{aligned} &|\psi_0^i\rangle = |n_d=1, n_f=0\rangle , \quad \epsilon_0^i = 0 , \\ &|\psi_{1\sigma}^i\rangle = |n_d=1, n_{f\sigma}=1\rangle , \quad \epsilon_1^i = \epsilon_f , \\ &|\psi_2^i\rangle = |n_d=1, n_f=2\rangle , \quad \epsilon_2^i = 2\epsilon_f + U_{ff} , \end{aligned} \quad (5)$$

while the final-state atomic limit configurations and energies are

$$\begin{aligned} &|\phi_0^F\rangle = |n_d=0, n_f=0\rangle , \quad \epsilon_0^f = -\epsilon_d , \\ &|\psi_{1\sigma}^F\rangle = |n_d=0, n_{f\sigma}=1\rangle , \\ &\epsilon_1^f = -\epsilon_d + \epsilon_f + U_{df} , \\ &|\psi_2^F\rangle = |n_d=0, n_f=2\rangle , \\ &\epsilon_2^f = -\epsilon_d + 2\epsilon_f + 2U_{df} + U_{ff} . \end{aligned} \quad (6)$$

If $V_{kf}$ is very small, the system will spend quite long periods of time in each of the initial configurations, following the Heisenberg uncertainty principle, so that an incoming x-ray photon may catch, temporarily, the system in one of the four configurations listed above [Eq. (5)]. On ejection of a photoelectron, a transition to the final states with different $f$ occupancy is possible, so we may expect in general to see spectral features corresponding to seven different "transition energies" in the first order of $V_{kf}$ (see Fig. 2):

$$
\begin{aligned}
E_{00}&=\epsilon_0^i-\epsilon_0^f=\epsilon_d\ ,\\
E_{01}&=\epsilon_0^i-\epsilon_1^f=\epsilon_d-\epsilon_f-U_{df}\ ,\\
E_{10}&=\epsilon_1^i-\epsilon_0^f=\epsilon_d+\epsilon_f\ ,\\
E_{11}&=\epsilon_1^i-\epsilon_1^f=\epsilon_d-U_{df}\ ,\\
E_{12}&=\epsilon_1^i-\epsilon_2^f=\epsilon_d-\epsilon_f-2U_{df}-U_{ff}\ ,\\
E_{21}&=\epsilon_2^i-\epsilon_1^f=\epsilon_d+\epsilon_f-U_{df}+U_{ff}\ ,\\
E_{22}&=\epsilon_2^i-\epsilon_2^f=\epsilon_d-2U_{df}\ .
\end{aligned}
\tag{7}
$$

Of course, these represent virtual transitions since the exact eigenstates of Eq. (1) will lead generally to a transition between a unique ground state ($n_d=1$) and a continuum of excited states ($n_d=0$). However, the above atomic limit transitions should become increasingly well defined as $V_{kf}\rightarrow 0$ so that they will define possible excitation energies at which the continuum should show enhanced features, albeit with spectral weights, some of which vary as a power of $V_{kf}$, hence are increasingly weak in this limit. As $V_{kf}$ increases, the above transitions will broaden and merge together into a general continuum, so this classification becomes less useful.

### B. Decoupling approximation

We calculate the Green's function $G_{dd}(\omega)$ by the equation-of-motion method[18,19]

$$
i\frac{\partial}{\partial t}G_{dd}^R(t)=\delta(t)-i\Theta(t)\langle\{[a_d(t),H],a_d^\dagger\}\rangle \tag{8}
$$

whose Fourier transform gives

$$
\omega G_{dd}(\omega)=1+\langle\langle[a_d,H];a_d^\dagger\rangle\rangle_\omega\ . \tag{9}
$$

Through the use of the model Hamiltonian of Eq. (1), we can evaluate these commutators and get the following equations of motion:

$$
(\omega-\epsilon_d)G_{dd}(\omega)=1-U_{df}\sum_\sigma\langle\langle a_d n_{f\sigma};a_d^\dagger\rangle\rangle_\omega\ , \tag{10}
$$

$$
\begin{aligned}
(\omega-\epsilon_d+U_{df})\langle\langle a_d n_{f\sigma};a_d^\dagger\rangle\rangle_\omega&=\langle n_{f\sigma}\rangle-U_{df}\langle\langle a_d n_{f\sigma}n_{f-\sigma};a_d^\dagger\rangle\rangle_\omega\\
&\quad-\sum_k V_{kf}(\langle\langle a_d a_{k\sigma}a_{f\sigma}^\dagger;a_d^\dagger\rangle\rangle_\omega+\langle\langle a_d a_{k\sigma}^\dagger a_{f\sigma};a_d^\dagger\rangle\rangle_\omega)\ ,
\end{aligned}
\tag{11}
$$

$$
\begin{aligned}
(\omega-\epsilon_d+2U_{df})\langle\langle a_d n_{f\sigma}n_{f-\sigma};a_d^\dagger\rangle\rangle_\omega&=\langle n_{f\sigma}n_{f-\sigma}\rangle-\sum_{k,\sigma'}V_{kf}(\langle\langle a_d n_{f-\sigma'}a_{k\sigma'}a_{f\sigma'}^\dagger;a_d^\dagger\rangle\rangle_\omega\\
&\quad+\langle\langle a_d n_{f-\sigma'}a_{k\sigma'}^\dagger a_{f\sigma'};a_d^\dagger\rangle\rangle_\omega)\ ,
\end{aligned}
\tag{12}
$$

where $\langle n_{f\sigma}\rangle$, $\langle n_{f\sigma}n_{f-\sigma}\rangle$ are ground-state expectation values, and the operator identity $n_{f\sigma}^2=n_{f\sigma}$ is used.

The higher-order Green's functions on the right-hand sides of Eqs. (11) and (12) cannot be expressed in terms of the lower-order Green's functions, and their equations of motion lead to still higher-order Green's functions, which do not form a closed set of equations. In order to proceed, we follow Hubbard,[18] Hewson,[17] and Hewson and Zuckerman[21] by decoupling the $k,k'$ electrons from $d$ hole and $f$ electron in the higher-order Green's functions resulting at the next level of the equations of motion in the following way:

$$
\begin{aligned}
&\langle\langle a_d a_{k'\sigma}^\dagger a_{k\sigma};a_d^\dagger\rangle\rangle_\omega\simeq\langle a_{k'\sigma}^\dagger a_{k\sigma}\rangle G_{dd}(\omega)=\delta_{kk'}\Theta(k_F-k)G_{dd}(\omega)\ ,\\
&\langle\langle a_d a_{k\sigma}^\dagger a_{k'\sigma};a_d^\dagger\rangle\rangle_\omega\simeq\langle a_{k\sigma}^\dagger a_{k'\sigma}\rangle G_{dd}(\omega)=\delta_{kk'}\Theta(k_F-k)G_{dd}(\omega)\ ,\\
&\langle\langle a_d a_{k'-\sigma}^\dagger a_{k\sigma}a_{f-\sigma}a_{f\sigma}^\dagger;a_d^\dagger\rangle\rangle_\omega\simeq\langle a_{k'-\sigma}^\dagger a_{k\sigma}\rangle\langle\langle a_d a_{f-\sigma}a_{f\sigma}^\dagger;a_d^\dagger\rangle\rangle_\omega=0\ ,\\
&\langle\langle a_d a_{k'\sigma}^\dagger a_{k\sigma}n_{f-\sigma};a_d^\dagger\rangle\rangle_\omega\simeq\langle a_{k'\sigma}^\dagger a_{k\sigma}\rangle\langle\langle a_d n_{f-\sigma};a_d^\dagger\rangle\rangle_\omega=\delta_{kk'}\Theta(k_F-k)\langle\langle a_d n_{f-\sigma};a_d^\dagger\rangle\rangle_\omega\ ,\\
&\langle\langle a_d a_{k'-\sigma}a_{k\sigma}a_{f\sigma}^\dagger a_{f-\sigma};a_d^\dagger\rangle\rangle_\omega\simeq\langle a_{k'-\sigma}a_{k\sigma}\rangle\langle\langle a_d a_{f\sigma}^\dagger a_{f-\sigma};a_d^\dagger\rangle\rangle_\omega=0\ ,\\
&\langle\langle a_d a_{k'-\sigma}^\dagger a_{k\sigma}^\dagger a_{f-\sigma}a_{f\sigma};a_d^\dagger\rangle\rangle_\omega\simeq\langle a_{k'-\sigma}^\dagger a_{k\sigma}^\dagger\rangle\langle\langle a_d a_{f-\sigma}a_{f\sigma};a_d^\dagger\rangle\rangle_\omega=0\ ,\\
&\langle\langle a_d a_{k\sigma}^\dagger a_{k'\sigma}n_{f-\sigma};a_d^\dagger\rangle\rangle_\omega\simeq\langle a_{k\sigma}^\dagger a_{k'\sigma}\rangle\langle\langle a_d n_{f-\sigma};a_d^\dagger\rangle\rangle_\omega=\delta_{kk'}\Theta(k_F-k)\langle\langle a_d n_{f-\sigma};a_d^\dagger\rangle\rangle_\omega\ ,\\
&\langle\langle a_d a_{k'-\sigma}a_{k\sigma}^\dagger a_{f-\sigma}^\dagger a_{f\sigma};a_d^\dagger\rangle\rangle_\omega\simeq\langle a_{k'-\sigma}a_{k\sigma}^\dagger\rangle\langle\langle a_d a_{f-\sigma}^\dagger a_{f\sigma};a_d^\dagger\rangle\rangle_\omega=0\ .
\end{aligned}
\tag{13}
$$

We have used here the fact that for a nondegenerate ground state with definite total $z$ component of spin, we have expectation values

$$\langle a^{\dagger}_{k'\sigma}a_{k\sigma}\rangle=\langle a^{\dagger}_{k\sigma}a_{k'\sigma}\rangle=\delta_{kk'}\Theta(k_F-k)\ ,$$
$$\langle a^{\dagger}_{k'-\sigma}a_{k\sigma}\rangle=\langle a_{k'-\sigma}a^{\dagger}_{k\sigma}\rangle=0\ ,\quad \langle a_{k'-\sigma}a_{k\sigma}\rangle=\langle a^{\dagger}_{k'-\sigma}a^{\dagger}_{k\sigma}\rangle=0\ , \tag{14}$$

in the lowest-order approximation.

This method of decoupling preserves intact all the Green's functions that involve the correlation energy $U_{df}$ between the core hole and $f$ electron and $U_{ff}$ between two $f$ electrons, and makes an approximation of order $V^2_{kf}$. Physically, this approximation fits nicely with the rare-earth mixed-valence compounds, where the parameters $U_{df}$, $U_{ff}$ (of order 10 eV) are much larger than $V_{kf}$ (of order 1 eV). Therefore, the effects of correlations are expected to be much more important than the hybridization. After some algebra, this decoupling scheme gives the following closed expression for $G_{dd}(\omega)$:

$$G_{dd}(\omega)=\frac{1-G_1[\langle n_{f\uparrow}+n_{f\downarrow}\rangle-\Pi_{kf}-\Pi_{fk}-2G_2(\langle n_{f\uparrow}n_{f\downarrow}\rangle-\Xi_2)]}{\omega-E_{00}-2\Lambda_{01}G_1}\ , \tag{15}$$

where

$$G_1=\frac{U_{df}}{\omega-E_{11}-(\Sigma_{01}+\Lambda_{01}-\Lambda_{12}+2\Lambda_{12}G_2)}\ ,$$

$$G_2=\frac{U_{df}}{\omega-E_{22}-2\Sigma_{12}}\ ,$$

$$\Sigma_{01}=\sum_k V^2_{kf}\left[\frac{1}{\omega-\epsilon_k-E_{01}}+\frac{1}{\omega+\epsilon_k-E_{10}}\right]\ ,$$

$$\Sigma_{12}=\sum_k V^2_{kf}\left[\frac{1}{\omega-\epsilon_k-E_{12}}+\frac{1}{\omega+\epsilon_k-E_{21}}\right]\ ,$$

$$\Lambda_{01}=\sum_{k<k_F} V^2_{kf}\left[\frac{1}{\omega-\epsilon_k-E_{01}}+\frac{1}{\omega+\epsilon_k-E_{10}}\right]\ ,$$

$$\Lambda_{12}=\sum_{k<k_F} V^2_{kf}\left[\frac{1}{\omega-\epsilon_k-E_{12}}+\frac{1}{\omega+\epsilon_k-E_{21}}\right]\ ,$$

$$\Pi_{kf}=\sum_{k\sigma} V_{kf}\left[\frac{\langle a_{k\sigma}a^{\dagger}_{f\sigma}\rangle-\langle a_{k\sigma}n_{f-\sigma}a^{\dagger}_{f\sigma}\rangle}{\omega-\epsilon_k-E_{01}}+\frac{\langle a_{k\sigma}n_{f-\sigma}a^{\dagger}_{f\sigma}\rangle}{\omega-\epsilon_k-E_{12}}\right]\ ,$$

$$\Pi_{fk}=\sum_{k\sigma} V_{kf}\left[\frac{\langle a^{\dagger}_{k\sigma}a_{f\sigma}\rangle-\langle a^{\dagger}_{k\sigma}n_{f-\sigma}a_{f\sigma}\rangle}{\omega+\epsilon_k-E_{10}}+\frac{\langle a^{\dagger}_{k\sigma}n_{f-\sigma}a_{f\sigma}\rangle}{\omega+\epsilon_k-E_{21}}\right]\ ,$$

$$\Xi_2=\sum_{k\sigma} V_{kf}\left[\frac{\langle a_{k\sigma}n_{f-\sigma}a^{\dagger}_{f\sigma}\rangle}{\omega-\epsilon_k-E_{12}}+\frac{\langle a^{\dagger}_{k\sigma}n_{f-\sigma}a_{f\sigma}\rangle}{\omega+\epsilon_k-E_{21}}\right]\ .$$

This result gives the correct limiting form Eq. (4) as $V_{kf}\to 0$. It may be seen that our principal result, Eq. (15), contains denominators which lead to enhancement of the spectrum at the virtual transition energies [Eq. (7)] as discussed above.

### C. Ground-state calculations

As we can see from the above expression for $G_{dd}(\omega)$, we now need the ground-state expectation values for $\langle n_{f\sigma}\rangle$, $\langle n_{f\sigma}n_{f-\sigma}\rangle$, $\langle a_{k\sigma}a^{\dagger}_{f\sigma}\rangle$, $\langle a^{\dagger}_{k\sigma}a_{f\sigma}\rangle$, $\langle a_{k\sigma}n_{f-\sigma}a^{\dagger}_{f\sigma}\rangle$, and $\langle a^{\dagger}_{k\sigma}n_{f-\sigma}a_{f\sigma}\rangle$. The expectation values can be expressed in terms of various Green's functions via the Lehmann representation as follows:

$$\langle n_{f\sigma}\rangle=-\frac{1}{\pi}\int_{-\infty}^{\mu}\mathrm{Im}G^{\sigma}_{ff}(\omega)d\omega\ , \tag{16}$$

$$\langle n_{f\sigma}n_{f-\sigma}\rangle=-\frac{1}{\pi}\int_{-\infty}^{\mu}\mathrm{Im}\Gamma^{\sigma}_{ff}(\omega)d\omega\ , \tag{17}$$

$$\langle a^{\dagger}_{k\sigma}a_{f\sigma}\rangle=-\frac{1}{\pi}\int_{-\infty}^{\mu}\mathrm{Im}G^{\sigma}_{fk}(\omega)d\omega\ , \tag{18}$$

$$\langle a_{k\sigma}a^{\dagger}_{f\sigma}\rangle=\frac{1}{\pi}\int_{-\infty}^{\mu}\mathrm{Im}G^{\sigma}_{kf}(\omega)d\omega\ , \tag{19}$$

$$\langle a^{\dagger}_{k\sigma}n_{f-\sigma}a_{f\sigma}\rangle=-\frac{1}{\pi}\int_{-\infty}^{\mu}\mathrm{Im}\Gamma^{\sigma}_{fk}(\omega)d\omega\ , \tag{20}$$

$$\langle a_{k\sigma}n_{f-\sigma}a^{\dagger}_{f\sigma}\rangle=\frac{1}{\pi}\int_{-\infty}^{\mu}\mathrm{Im}\Gamma^{\sigma}_{kf}(\omega)d\omega\ , \tag{21}$$

where $\mu$ is the chemical potential (the Fermi energy $E_F$ in this case). Equations (18)—(20) result from an assumption that

$$G^{\sigma}_{kf}=G^{\sigma}_{fk},\quad \Gamma^{\sigma}_{kf}=\Gamma^{\sigma}_{fk}\ , \tag{22}$$

and are not generally true.

The above Green's functions are defined as

$$G^{\sigma}_{ff}(\omega)\equiv\langle\langle a_{f\sigma};a^{\dagger}_{f\sigma}\rangle\rangle_{\omega}\ ,$$
$$G^{\sigma}_{fk}(\omega)\equiv\langle\langle a_{f\sigma};a^{\dagger}_{k\sigma}\rangle\rangle_{\omega}\ ,$$
$$G^{\sigma}_{kf}(\omega)\equiv\langle\langle a_{k\sigma};a^{\dagger}_{f\sigma}\rangle\rangle_{\omega}\ ,$$
$$\Gamma^{\sigma}_{ff}(\omega)\equiv\langle\langle a_{f\sigma}n_{f-\sigma};a^{\dagger}_{f\sigma}\rangle\rangle_{\omega}\ ,$$
$$\Gamma^{\sigma}_{fk}(\omega)\equiv\langle\langle a_{f\sigma}n_{f-\sigma};a^{\dagger}_{k\sigma}\rangle\rangle_{\omega}\ ,$$
$$\Gamma^{\sigma}_{kf}(\omega)\equiv\langle\langle a_{k\sigma}n_{f-\sigma};a^{\dagger}_{f\sigma}\rangle\rangle_{\omega}\ .$$

To get these Green's functions $G^{\sigma}_{ff}(\omega)$, $G^{\sigma}_{fk}(\omega)$, $\Gamma^{\sigma}_{ff}(\omega)$, $\Gamma^{\sigma}_{fk}(\omega)$ in the ground state, we again use the equation-of-motion method, this time in the absence of the core hole [$n_d=1$ in Eq. (1)] so that the $U_{df}$ term does not enter. We follow the same decoupling scheme as in Eq. (13), leading to neglect of correlations between $k,k'$ states and $f$ states. This decoupling scheme was used by Hewson and Zuckermann[21] in studying the ground-state properties of the Anderson-model Hamiltonian, and they showed that it gives a nonmagnetic ground state. In addition, this decoupling scheme is consistent with the assumptions [Eq. (22)] used above.

This approximation gives the following simple expressions for the Green's functions:

$$G^{\sigma}_{ff}(\omega)=\frac{1-\langle n_{f-\sigma}\rangle}{\omega-\epsilon_f-\Sigma_0(\omega)}+\frac{\langle n_{f-\sigma}\rangle}{\omega-\epsilon_f-U_{ff}-\Sigma_0(\omega)}\ , \tag{23}$$

$$G^{\sigma}_{kf}(\omega)=G^{\sigma}_{fk}(\omega)=\frac{V_{kf}}{\omega-\epsilon_k}G^{\sigma}_{ff}(\omega)\ , \tag{24}$$

$$\Gamma^{\sigma}_{ff}(\omega)=\frac{\langle n_{f-\sigma}\rangle}{\omega-\epsilon_f-U_{ff}-\Sigma_0(\omega)}\ , \tag{25}$$

$$\Gamma^{\sigma}_{kf}(\omega)=\Gamma^{\sigma}_{fk}(\omega)=\frac{V_{fk}}{\omega-\epsilon_k}\Gamma^{\sigma}_{ff}(\omega)\ , \tag{26}$$

where

$$\Sigma_0(\omega)=\sum_{k'}\frac{V^2_{fk'}}{\omega-\epsilon_{k'}}\ . \tag{27}$$

We note that $G^{\sigma}_{kf}(\omega)=G^{\sigma}_{fk}(\omega)$ and $\Gamma^{\sigma}_{kf}(\omega)=\Gamma^{\sigma}_{fk}(\omega)$ as assumed above.

The density of states of the $f$ level in this approximation gives a very intuitive interpretation.

$$\rho^{\sigma}_f(E)=-\frac{1}{\pi}\mathrm{Im}G^{\sigma}_{ff}(E)=\frac{1}{\pi}\left[\frac{(1-\langle n_{f-\sigma}\rangle)\Delta}{(E-\epsilon_f-\Lambda)^2+\Delta^2}+\frac{\langle n_{f-\sigma}\rangle\Delta}{(E-\epsilon_f-U_{ff}-\Lambda)^2+\Delta^2}\right], \tag{28}$$

where we have set

$$\Sigma_0(\omega)=\Lambda(\omega)-i\Delta(\omega)\ . \tag{29}$$

This simply describes the two $f$ levels $\epsilon_f$ and $\epsilon_f+U_{ff}$ broadened and shifted due to the mixing potential $V_{fk}$. The respective spectral weights depend on the occupation number of the opposite spin state.

The ground-state expectation values given by Eqs. (23)–(27) are

$$\langle n_{f\sigma}\rangle=(1-\langle n_{f-\sigma}\rangle)\frac{1}{\pi}\int_{-B}^{\mu}d\omega\frac{\Delta}{(\omega-\epsilon_f-\Lambda)^2+\Delta^2}+\langle n_{f-\sigma}\rangle\frac{1}{\pi}\int_{-B}^{\mu}d\omega\frac{\Delta}{(\omega-\epsilon_f-U_{ff}-\Lambda)^2+\Delta^2}\ , \tag{30}$$

$$\langle n_{f\sigma}n_{f-\sigma}\rangle=\langle n_{f-\sigma}\rangle\frac{1}{\pi}\int_{-B}^{\mu}d\omega\frac{\Delta}{(\omega-\epsilon_f-U_{ff}-\Lambda)^2+\Delta^2}\ ,$$

$$\langle a^{\dagger}_{k\sigma}a_{f\sigma}\rangle=-\langle a_{k\sigma}a^{\dagger}_{f\sigma}\rangle=(1-\langle n_{f-\sigma}\rangle)\left[\Theta(-\epsilon_k)V_{fk}\frac{(\epsilon_k-\epsilon_f-\Lambda)}{(\epsilon_k-\epsilon_f-\Lambda)^2+\Delta^2}+\frac{V_{fk}}{\pi}\int_{-B}^{\mu}P\frac{d\omega}{(\omega-\epsilon_k)}\frac{\Delta}{(\omega-\epsilon_f-\Lambda)^2+\Delta^2}\right]$$

$$+\langle n_{f-\sigma}\rangle\left[\Theta(-\epsilon_k)V_{fk}\frac{(\epsilon_k-\epsilon_f-U_{ff}-\Lambda)}{(\epsilon_k-\epsilon_f-U_{ff}-\Lambda)^2+\Delta^2}+\frac{V_{fk}}{\pi}\int_{-B}^{\mu}P\frac{d\omega}{(\omega-\epsilon_k)}\frac{\Delta}{(\omega-\epsilon_f-U_{ff}-\Lambda)^2+\Delta^2}\right],$$

$$\langle a^{\dagger}_{k\sigma}n_{f-\sigma}a_{f\sigma}\rangle=-\langle a_{k\sigma}n_{f-\sigma}a^{\dagger}_{f\sigma}\rangle=\langle n_{f-\sigma}\rangle V_{fk}\left[\Theta(-\epsilon_k)\frac{(\epsilon_k-\epsilon_f-U_{ff}-\Lambda)}{(\epsilon_k-\epsilon_f-U_{ff}-\Lambda)^2+\Delta^2}+\frac{1}{\pi}\int_{-B}^{\mu}P\frac{d\omega}{(\omega-\epsilon_k)}\frac{\Delta}{(\omega-\epsilon_f-U_{ff}-\Lambda)^2+\Delta^2}\right],$$

where $P(1/\omega-\epsilon_k)$ represents the principal value, $B$ is the conduction-band width, and we used the fact that

$\Delta(\omega)=0$ outside $B$. The $f$ level occupation number $\langle n_{f\sigma}\rangle$ is, in general, given by the self-consistent solution of two simultaneous equations generated by Eq. (30) for $\langle n_{f\uparrow}\rangle$ and $\langle n_{f\downarrow}\rangle$. In this case, however, we have only one simple algebraic equation to solve since it is known that it has only a nonmagnetic solution $\langle n_{f\uparrow}\rangle=\langle n_{f\downarrow}\rangle$. Equation (15), together with these ground-state expectation values, gives $G_{dd}(\omega)$ in this decoupling approximation.

## III. RESULTS AND DISCUSSION

We now apply these results to some cases of interest. We set $U_{ff}=6$ eV and $U_{df}=-10$ eV corresponding to the values obtained from XPS data on Ce compounds by Lässer *et al.*[22] We also assume $V_{kf}=V$ for simplicity. Following SG,[12] we consider a half-filled semielliptical metal band of width $B$, whose density of states is given by

$$\rho(\epsilon)=\frac{2}{\pi}\frac{1}{B^2}(B^2-\epsilon^2)^{1/2}\ . \tag{31}$$

Then the real and imaginary parts of the self-energy Eq. (29) can be computed from the relation

$$\int_{-B}^{B}\frac{\rho(\epsilon_k)}{(x\pm\epsilon_k)}d\epsilon_k=\begin{cases}\dfrac{2}{x+(x^2-B^2)^{1/2}} & \text{if } x>B\\ \dfrac{2x}{B^2}-i\dfrac{2}{B^2}(B^2-x^2)^{1/2} & \text{if } -B\le x\le B\\ \dfrac{2}{x-(x^2-B^2)^{1/2}} & \text{if } x<-B\end{cases}$$

which gives

$$\Lambda(\omega)=\frac{2V^2}{B^2}\omega,\quad \Delta(\omega)=\frac{2V^2}{B^2}(B^2-\omega^2)^{1/2}\ , \tag{32}$$

for $-B\le\omega\le B$ (within the conduction band).

We also include the lifetime of a core hole by substituting $\epsilon_d-i\gamma$ in place of $\epsilon_d$ in the above formulas in order to mimic the effect of lifetime broadening due to residual Coulomb interactions such as Auger processes. Mathematically this also prevents the integrals from diverging. We set $B=3$ eV and $\gamma=0.3$ eV in the following calculations, and we smoothed out the curves in the figures by convoluting them with a Lorentzian broadening function of half-width 0.1 eV.

Unfortunately, we find that for $V_{kf}\gtrsim 0.5$ eV, $\mathrm{Im}G_{dd}(\omega)$ starts to go negative for a certain range of $\omega$ values, indicating that the decoupling approximation does not conserve probability at each value of $\omega$. However, in each of the cases presented below (for $V_{kf}$ up to 0.9 eV) we integrated out the total area under all the peaks as a consistency check, and found it always comes out very close to unity, indicating that the calculation preserves probability overall and may be expected to give a reasonable estimate of the transfer of spectral weight between the various peaks without adding spurious unphysical peaks.

In Fig. 3, we show the calculated core-level spectra for the case of $\epsilon_f=1.5$ eV corresponding to $\langle n_f\rangle\lesssim 0.12$ (depending on $V$), i.e., an initially almost empty $f$ state. As we increase $V$ from 0.1 to 0.9 ($U_{df}=-10$ eV, $U_{ff}=6$ eV), we see that the well-screened peak ($f^{n+1}$ configuration) at $\omega-\epsilon_d\simeq 8.5$ eV grows as $V$ is increased, just as SG observed. However, the parameters here are such that the unscreened peak is still much stronger.

The mixed-valence case with initial valence 0.5 is shown in Fig. 4 for values of $V$ from 0.1 to 0.9 (again $U_{df}=-10$ eV, $U_{ff}=6$ eV). In these curves, the parameter $\epsilon_f$ is varied for each $V$ to find the value for which

$$\sum_{\sigma}(\langle n_{f\sigma}\rangle-\langle n_{f\uparrow}n_{f\downarrow}\rangle)=0.5\ .$$

($\langle n_{f\uparrow}n_{f\downarrow}\rangle$ is in fact negligible for the present cases.) We see that for large $V$ ($V=0.7$, 0.9) a new peak at about 13.5 eV begins to show up. We assign this new peak to a shake-down structure with a $f^{n+2}$ final state. This comes about because the effective energy level of the spin-up $f$ electron

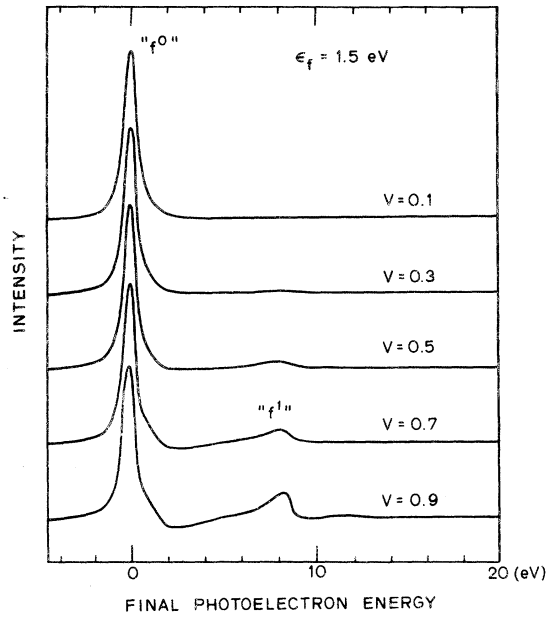


FIG. 3. A series of core-level spectra with $\epsilon_f=1.5$, $U_{ff}=6.0$, $U_{df}=-10.0$, $B=3.0$ as $V$ is increased from 0.1 to 0.9. We see the growth of the well-screened peak at about 8.5 eV. Initial values of $\langle n_f\rangle$ are $\lesssim 0.01$ for $V=0.1$ and 0.3, and 0.04, 0.08, 0.12 for $V=0.5$, 0.7, 0.9, respectively.

when the spin-down $f$ level is occupied is $\epsilon_f+U_{df}+U_{ff}$ (about 3.7 eV in the case of $V=0.9$) below the Fermi level as shown in Fig. 1, so that the system gains more energy by occupying both $f$ levels. As $V$ is increased, we also see the transfer of spectral weight from the unscreened peak ($f^0$) to the well-screened peak ($f^1$,$f^2$). In Fig. 5 we plot the relative weight of each peak as $V$ is varied. As may be seen, the well-screened peak gains spectral weight with increasing $V$. The shake-down effect gives a discrepancy of order 0.1 in the estimate of the ground-state valence from the core-level photoemission in the strongest hybridization case we have looked at ($V=0.9$) with the present parameters $U_{df}=-10$ eV, and $U_{ff}=6$ eV.

The fact that the shake-down effect is relatively weak for the case of $V \ll |U_{df}|$ can be understood qualitatively by considering the zero-bandwidth limit ($B=0$). In this simple case of two states with hybridization $V$ between them, we have the initial ground-state wave function $\psi_i$ with $\langle n_f\rangle=0.5$,

$$|\psi_i\rangle=\frac{1}{\sqrt{2}}(|n_f=0\rangle-|n_f=1\rangle)\,.$$

(Here we neglect the contribution of the $|n_f=2\rangle$ state, since it is of higher order in $V$ than the one

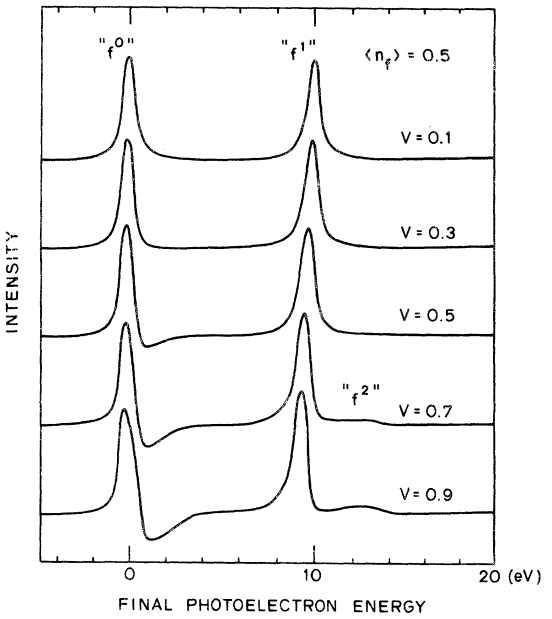


FIG. 4. Core-level spectra for the mixed-valence case. Parameters are $U_{ff}=6.0$, $U_{df}=-10.0$, $B=3.0$ as before, and $\epsilon_f$ is adjusted to $V$ to give the initial valence of 0.5. Values of $\epsilon_f$ are 0.0038, 0.034, 0.091, 0.172, and 0.27 for $V=0.1$, 0.3, 0.5, 0.7, and 0.9, respectively. Final photoelectron energy is measured relative to the unscreened peak, i.e., $\epsilon_k=\hbar\omega_q-|\epsilon_d|$. The dip around 1 eV is an artifact of the decoupling approximation, and is not real.

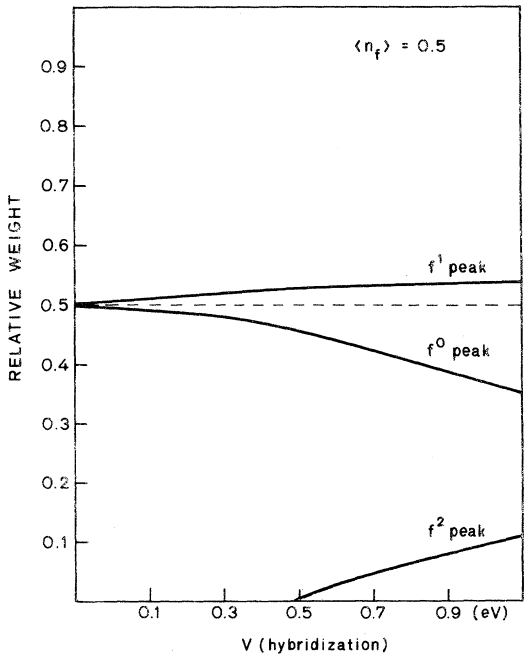


FIG. 5. Areas under the $f^0$,$f^1$,$f^2$ peaks in Fig. 4 as the hybridization is increased from $V=0.1$ to 0.9. Initial ground-state valence is 0.5, indicated by the dashed line.

being considered.)

In the final state, the unscreened state with a predominantly $|n_f=0\rangle$ component has wave function $\psi_f$:

$$|\psi_f\rangle=\left[|n_f=0\rangle-\frac{\sqrt{2}V}{U_{df}}|n_f=1\rangle\right].$$

Since the intensity of this peak in the photoemission spectra is given by the square of its overlap with the ground-state wave function, we get the intensity of the unscreened peak equal to $(1/\sqrt{2}+V/U_{df})^2$. Hence, we see that the shake-down effect, in the lowest order in $V$, is of the order of $|V/U_{df}|$. For the parameters considered with $V=0.9$, this gives $|V/U_{df}|\simeq 1/10\simeq 0.1$, as observed in Fig. 5.

Similar trends in shift of spectral weight are observed in other values of initial valence $\langle n_f\rangle$. In Fig. 6 are shown the relative weights of the $f^0,f^1,f^2$ peaks for the cases of $\langle n_f\rangle=0.1$ and 0.9 as the hybridization is increased from $V=0.1$ to 0.9. The qualitative trend of the shift of spectral weight from the unscreened peak to the screened peak is again evident, but we note that in the case of $\langle n_f\rangle=0.9$ the shift is primarily from the $f^1$ to the $f^2$ peak rather than from the $f^0$ to the $f^1$ peak. In general, the amount of spectral weight transfer from the $f^n$ to the $f^{n+1}$ peak will not be the same as that from the $f^{n+1}$ to the $f^{n+2}$ peak.

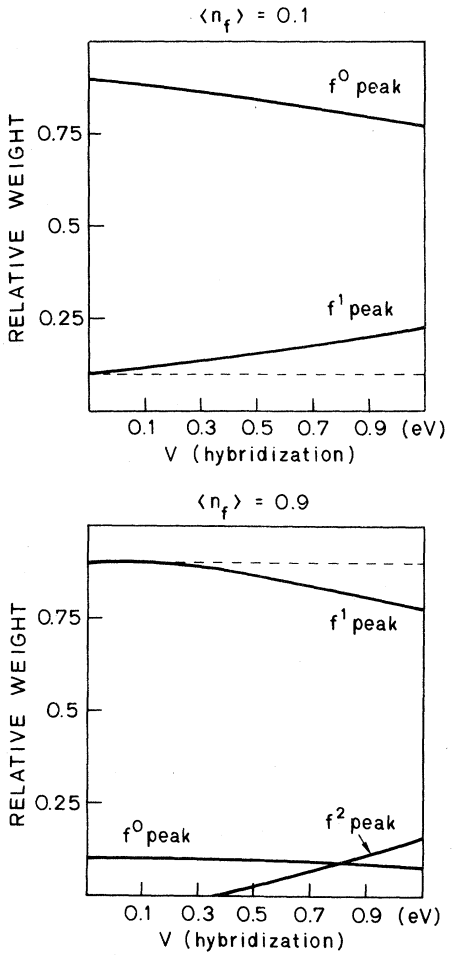


FIG. 6. Spectral weights of $f^0,f^1,f^2$ peaks for the cases of initial valence $\langle n_f\rangle=0.1$ and 0.9 as a function of hybridization. Parameters are the same as in Fig. 4, except that $\epsilon_f$ is varied to give the desired initial ground-state valence.

## IV. CONCLUDING REMARKS

From the measured ratio of intensities for final $f^n$ and $f^{n+1}$ states in $CePd_3$ XPS data, we should deduce a ground-state valence of 3.1 in the spectator-hole limit.[22] However, other data (e.g., lattice constant) indicate that the $CePd_3$ ground-state valence is of order 3.4.[23] From Fig. 5, it may be seen that at $V_{fk}$ of order 0.9 eV, the apparent $f^0$ occupation number is reduced from a ground-state value of 0.5 to an apparent value of 0.4. It seems likely that, on extrapolation of the curve in Fig. 5, a value of $V_{fk}\cong 1.5$ eV would be sufficient to resolve the above apparent discrepancy. This would be in rough agreement with resonant photoemission data.[5] However, our calculation can only be taken in a qualitative sense at such large values of $V_{kf}$. Our principal conclusion, therefore, is that observed final-state effects require a much stronger $k$-$f$ hybridization than the $\sim 10$ meV believed some years ago. Hence, the hybridization is strong enough that a simple "atomic limit" estimate of the ground-state valence using XPS and neglecting final-state effects is unreliable.

### *Note added in proof*

For the case of $CeRh_3$ mentioned in the Introduction, the intensity of the $f^1$ peak in the core-level XPS spectra[10] is too strong to be consistent with the tetravalent ground-state configuration and our estimate of the final-state screening effect, unless the hybridization is anomalously strong. Therefore it is likely that $CeRh_3$, and some other standard "tetravalent" Ce compounds with similar XPS spectra (e.g., $CeRu_2$,$CeCo_2$), are in fact

mixed-valent, not tetravalent as previously believed. This conclusion is supported by recent resonant valence-band photoemission studies.[24,25]

The fact that screening effect is more important as $V$ is increased has been confirmed by the x-ray absorption edge measurement on Tm and Ce compounds. Bianconi *et al.*[26,27] found that for Tm compounds, where $V$ is small, the valence deduced from the x-ray edge structure is in good agreement with other estimates (e.g., volume or magnetic moment), while for Ce compounds the two valence estimates give some discrepancies. This is consistent with our main conclusion that for small $V$ a simple "spectator-hole" limit estimate using XPS core-level spectra may be reasonable, but for larger $V$ the effect of screening has to be taken into account.

## ACKNOWLEDGMENTS

We thank Professor I. Lindau for his support during the course of this work, and Dr. J. W. Allen for helpful discussions. This work is supported in part by the National Science Foundation under Contract No. DMR 79-13102.

---

*Present address: Xerox Palo Alto Research Center, Palo Alto, CA 94304.

[1]Y. Baer and Ch. Zürcher, Phys. Rev. Lett. 39, 956 (1977).

[2]Y. Baer, R. Hauger, Ch. Zürcher, M. Campagna, and G. K. Wertheim, Phys. Rev. B 18, 4433 (1978).

[3]J. -N. Chazalviel, M. Campagna, G. K. Wertheim, and P. H. Schmidt, Phys. Rev. B 14, 4586 (1976).

[4]J. W. Allen, L. I. Johansson, I. Lindau, and S. B. Hagström, Phys. Rev. B 21, 1335 (1980).

[5]J. W. Allen, S.-J. Oh, I. Lindau, J. M. Lawrence, L. I. Johansson, and S. B. Hagström, Phys. Rev. Lett. 46, 1100 (1981).

[6]G. K. Wertheim, in *Valence Fluctuations in Solids,* edited by L. M. Falicov, W. Hanke, and M. B. Maple (North-Holland, Amsterdam, 1981), p. 67.

[7]G. K. Wertheim, R. L. Cohen, A. Rosencwaig, and H. J. Guggenheim, in *Electron Spectroscopy,* edited by D. A. Shirley (North-Holland, Amsterdam, 1972), p. 813.

[8]G. Crecelius, G. K. Wertheim, and D. N. E. Buchanan, Phys. Rev. B 18, 6519 (1978).

[9]D. K. Wohlleben, in *Valence Fluctuations in Solids,* edited by L. M. Falicov, W. Hanke, and M. B. Maple (North-Holland, Amsterdam, 1981), p. 1.

[10]G. Krill, J.-P. Kappler, A. Meyer, L. Abadli, and M.-F. Ravet, in *Valence Fluctuations in Solids,* edited by L. M. Falicov, W. Hanke, and M. B. Maple (North-Holland, Amsterdam , 1981) p. 435.

[11]A. Kotani, and Y. Toyozawa, Jpn. J. Phys. 35, 1073 (1973); 35, 1082 (1973); 37, 912 (1974).

[12]K. Schönhammer and O. Gunnarsson, Solid State Commun. 23, 691 (1977); 26, 147 (1978); 26, 399 (1978); Z. Phys. B 30, 297 (1978).

[13]N. D. Lang and A. R. Williams, Phys. Rev. B 16, 2408 (1977).

[14]J. W. Gadzuk and S. Doniach, Surf. Sci. 77, 427 (1978).

[15]S. S. Hussain and D. M. Newns, Solid State Commun. 25, 1049 (1978).

[16]J. C. Fuggle, M. Campagna, Z. Zolnierek, R. Lässer, A. Platau, Phys. Rev. Lett. 45, 1597 (1980).

[17]Green's-function decoupling approximations have been used before by various authors. See, for example, Ref. 18, and also A. C. Hewson, Phys. Rev. 144, 420 (1966); Phys. Lett. 19, 5 (1965).

[18]J. Hubbard, Proc. R. Soc. London Ser. A 276, 238 (1963); 277, 237 (1964); 281, 401 (1964).

[19]D. N. Zubarev, Usp. Fiziol. Nauk 71, 71 (1960) [Sov. Phys.—Usp. 3, 320 (1960)].

[20]See, for example, S. Donaich and E. H. Sondheimer, *Green's Functions for Solid-State Physicists* (Benjamin, Reading, Massachusetts, 1974).

[21]A. C. Hewson and M. J. Zuckermann, Phys. Lett. 20, 219 (1966).

[22]R. Lässer, J. C. Fuggle, M. Beyss, M. Campagna, F. Steglich, and F. Hulliger, Physica (Utrecht) 102B, 360 (1980).

[23]J. M. Lawrence, P. S. Riseborough, and R. D. Parks, Rep. Prog. Phys. 44, 1 (1981).

[24]D. J. Peterman, J. H. Weaver, and M. Croft, Phys. Rev. B 25, 5530 (1982).

[25]J. W. Allen, S.-J. Oh, I. Lindau, M. B. Maple, J. F. Suassuna, and S. B. Hagström, Phys. Rev. B (in press).

[26]A. Bianconi, M. Campagna, and S. Stizza, Phys. Rev. B 25, 2477 (1982).

[27]A. Bianconi, S. Modesti, M. Campagna, K. Fischer, and S. Stizza, J. Phys. C 14, 4737 (1981).